Demonstration of a Controlled-Phase Gate for Continuous-Variable One-Way Quantum Computation

Ryuji Ukai,[1] Shota Yokoyama,[1] Jun-ichi Yoshikawa,[1] Peter van Loock,[2,3] and Akira Furusawa[1]

[1]*Department of Applied Physics, School of Engineering, The University of Tokyo, 7-3-1 Hongo, Bunkyo-ku, Tokyo 113-8656, Japan*

[2]*Optical Quantum Information Theory Group, Max Planck Institute for the Science of Light, Günther-Scharowsky-Strasse 1/Bau 26, 91058 Erlangen, Germany*

[3]*Institute of Theoretical Physics I, Universität Erlangen-Nürnberg, Staudtstrasse 7/B2, 91058 Erlangen, Germany*

(Received 3 July 2011; published 13 December 2011)

We experimentally demonstrate a controlled-phase gate for continuous variables using a cluster-state resource of four optical modes. The two independent input states of the gate are coupled with the cluster in a teleportation-based fashion. As a result, one of the entanglement links present in the initial cluster state appears in the two unmeasured output modes as the corresponding entangling gate acting on the input states. The genuine quantum character of this gate becomes manifest and is verified through the presence of entanglement at the output for a product two-mode coherent input state. By combining our gate with the recently reported module for single-mode Gaussian operations [R. Ukai *et al.*, Phys. Rev. Lett. **106**, 240504 (2011)], it is possible to implement any multimode Gaussian operation as a fully measurement-based one-way quantum computation.

DOI: 10.1103/PhysRevLett.107.250501 PACS numbers: 03.67.Lx, 42.50.Dv, 42.50.Ex

The one-way model of measurement-based quantum computation [1] is a fascinating alternative to the standard unitary-gate-based circuit model, for qubits as well as for continuous-variable (CV) encodings [2–4]. Such one-way schemes are realized through single-qubit or single-mode measurements together with outcome-dependent feedforward operations on a preprepared multiparty entangled state, the so-called "cluster state." By choosing an appropriate set of measurement bases on a sufficiently large cluster, an arbitrary unitary operation can be implemented for the corresponding encoding.

Prior to an actual extension of the one-way model from qubits to continuous variables, a CV analogue to qubit cluster states was proposed [2]. Subsequently, the notion of an in-principle universality of CV one-way quantum computation was proven on the assumptions of sufficiently long measurement-based gate sequences [5] and perfectly squeezed optical cluster-state resources, as well as the inclusion of at least one nonlinear, non-Gaussian measurement device [3]. Only shortly thereafter, by using squeezed vacuum states and beam splitters [6], various cluster states were generated in the lab [7,8]. Among these was the four-mode linear cluster state which would allow us to implement arbitrary single-mode Gaussian operations [9,10]. However, in order to demonstrate such single-mode gate operations on arbitrary input states, the input mode has to be attached to the cluster state. For a single quadratic gate, this can be accomplished using two squeezed-state ancillae, as described in Ref. [11]. A much simpler and more general solution [10], however, would employ a multimode measurement such as a Bell measurement, similar to standard CV quantum teleportation [12]. By using a four-mode linear cluster state and a Bell-measurement-based input coupling, a typical set of single-mode Gaussian operations such as squeezing and Fourier transformations was recently experimentally demonstrated [13].

The final missing element towards implementing arbitrary multimode Gaussian transformations in a one-way fashion [10] is a universal two-mode entangling gate. In fact, universal multimode operations (even including non-Gaussian ones) are, in an asymptotic sense, realizable when universal single-mode gates (including at least one non-Gaussian gate) are combined with any kind of quadratic (Gaussian) interaction gate [5]. For example, certain nonlinear multimode Hamiltonians such as a fairly strong two-mode cross-Kerr interaction would only require applying tens of quadratic and cubic single-mode gates, in addition to the two-mode controlled-phase (C_Z) gate [14]. More specifically, an arbitrary multimode Gaussian operation can be exactly recast as a finite decomposition into single-mode Gaussian gates and a quadratic (Gaussian) two-mode gate [5,10,15,16]. The most natural and easily implementable two-mode gate in this setting would be that corresponding to a vertical link between two individual modes of a CV cluster state—the C_Z gate [3]. Very recently, Wang *et al.* reported an attempt to experimentally demonstrate this gate [17]. However, the cluster state in that experiment was not of sufficient quality in order to operate the gate as a genuine nonclassical entangling gate; in fact, the two-mode input quantum state was degraded by such a large excess noise that no entanglement at all was present at the output.

In this Letter, we demonstrate a CV cluster-based C_Z gate operating in the quantum realm. In order to verify its

 © 2011 American Physical Society

nonclassicality, we show that the two-mode output state is indeed entangled when the input state is a product of two single-mode coherent states. Furthermore, several manifestations of the general input-output relation of the gate are realized, using various distinct coherent states as the input of the gate. The resource state is a four-mode linear cluster state, as illustrated in Fig. 1(a). Two independently prepared input coherent states are attached to the cluster state through beam splitters and, subsequently, homodyne detections are applied on the individual modes. This input-to-cluster coupling plus detection corresponds to a two-mode Bell measurement like in CV quantum teleportation [10], similar to those teleportation-based gates for qubits [18,19]. However, note that a fully measurement-controlled evolution is still possible by rotating each one-mode homodyne quadrature basis [10], or even replacing it by a nonhomodyne projection measurement. Similarly, this CV entangling gate could be directly incorporated into a one-way quantum computation of larger scale, see Fig. 1(b) [20]. Though not demonstrated here, on-off control of the entangling gate can be achieved by two additional vertices [see Fig. 1(c)] [21].

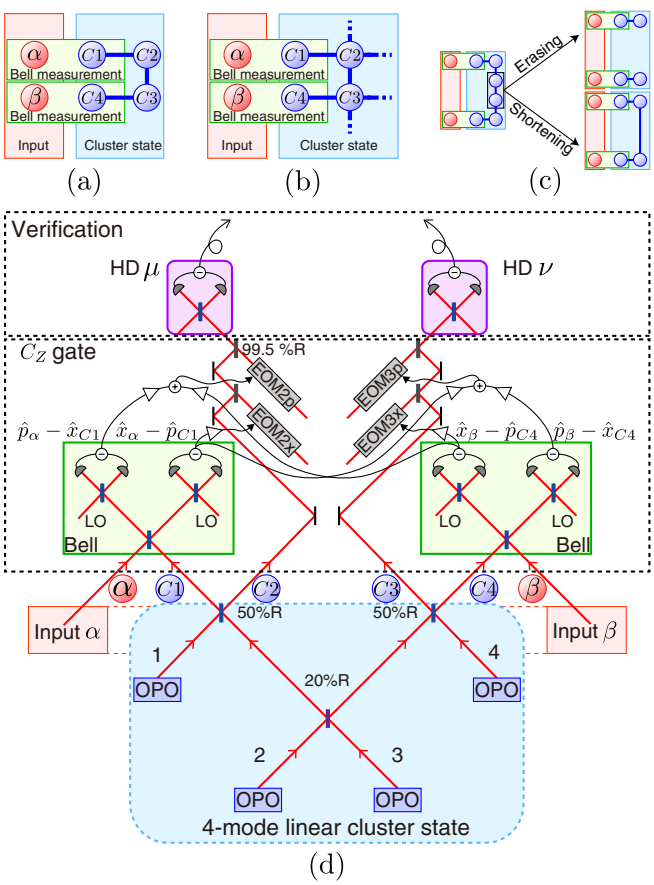

FIG. 1 (color online). (a) An abstract illustration of our experiment. (b) Input coupling through quantum teleportation for larger one-way quantum computations. (c) Cluster shaping. (d) A schematic of our experimental setup. OPO, optical parametric oscillator; LO, local oscillator for homodyne measurement; EOM, electro-optical modulator; HD, homodyne detection; Bell, Bell measurement.

In the following, we shall use the canonical position and momentum operators, $\hat{x}_j$ and $\hat{p}_j$, where the subscript j denotes an optical mode and $[\hat{x}_j, \hat{p}_k] = i\delta_{jk}/2$. The CV C_Z gate corresponds to the unitary operator $\hat{C}_{Zjk} = e^{2i\hat{x}_j\hat{x}_k}$ with the input-output relation,

$$\hat{\boldsymbol{\xi}}'_{jk} = \begin{pmatrix} I & S \\ S & I \end{pmatrix} \hat{\boldsymbol{\xi}}_{jk}, \tag{1}$$

where $\hat{\boldsymbol{\xi}}_{jk} = (\hat{x}_j, \hat{p}_j, \hat{x}_k, \hat{p}_k)^T$,

$$S = \begin{pmatrix} 0 & 0 \\ 1 & 0 \end{pmatrix}, \tag{2}$$

and I is the 2×2 identity matrix.

We demonstrate this C_Z gate by using a four-mode linear cluster state [$C1$-$C2$-$C3$-$C4$ in Fig. 1(a)]. A CV cluster state is defined, in the ideal case, through its zero eigenvalues for certain linear combinations of the canonical operators, $\hat{p}_{Cj} - \sum_{k\in N_j} \hat{x}_{Ck} (\equiv \hat{\delta}_j)$. Here, N_j denotes the set of nearest-neighbor modes of mode j, when the state is represented by a graph; see Figs. 1(a) and 1(b). The four-mode linear cluster state can be interpreted as two Einstein-Podolsky-Rosen (EPR) pairs ($C1$-$C2$ and $C3$-$C4$) with a C_Z interaction between them ($C2$-$C3$), up to local phase rotations. When two input states encoded in modes α and β are teleported to modes $C2$ and $C3$, using the double instance of EPR states, the initial C_Z interaction between the two EPR pairs is teleported onto the two input states [20].

Let us describe the above procedure for a nonideal, finitely squeezed cluster state corresponding to nonzero variances for the operators $\hat{\delta}_j$. When a four-mode linear cluster state is generated by using four finitely squeezed states and three beam splitters as in Fig. 1(d), the excess noises are as follows: $\hat{\delta}_1 = \sqrt{2}e^{-r}\hat{p}_1^{(0)}$, $\hat{\delta}_2 = -\frac{5}{\sqrt{10}}e^{-r} \times \hat{p}_3^{(0)} - \frac{1}{\sqrt{2}}e^{-r}\hat{p}_4^{(0)}$, $\hat{\delta}_3 = \frac{1}{\sqrt{2}}e^{-r}\hat{p}_1^{(0)} - \frac{5}{\sqrt{10}}e^{-r}\hat{p}_2^{(0)}$, and $\hat{\delta}_4 = -\sqrt{2}e^{-r}\hat{p}_4^{(0)}$, where $e^{-r}\hat{p}_j^{(0)}$ is the squeezed quadrature of the jth squeezed state. Here, we assume identical squeezing levels with parameter r for simplicity. Note that the limit $r \to \infty$ corresponds to an ideal cluster state. Two pairs of modes, $(\alpha, C1)$ and $(\beta, C4)$, are then subject to Bell measurements. For this purpose, four observables, $\hat{p}_\alpha - \hat{x}_{C1}$, $\hat{x}_\alpha - \hat{p}_{C1}$, $\hat{p}_\beta - \hat{x}_{C4}$, and $\hat{x}_\beta - \hat{p}_{C4}$, are measured, giving the measurement results t_α, t_1, t_β, and t_4, respectively. Then the corresponding feedforward operations $\hat{X}_{C2}(t_1)\hat{Z}_{C2}(t_\alpha + t_4)\hat{X}_{C3}(t_4)\hat{Z}_{C3}(t_\beta + t_1)$ are performed on modes $C2$ and $C3$, where $\hat{X}_j(s) = e^{-2is\hat{p}_j}$ and $\hat{Z}_j(s) = e^{2is\hat{x}_j}$ are the position and momentum displacement operators. The resulting position and momentum operators of modes $C2$ and $C3$ at the output, labeled by μ and ν, can then be written as

$$\hat{\boldsymbol{\xi}}_{\mu\nu} = \begin{pmatrix} I & S \\ S & I \end{pmatrix} \hat{\boldsymbol{\xi}}_{\alpha\beta} + \hat{\boldsymbol{\delta}}. \tag{3}$$

This completes the C_Z operation. Here, $\hat{\boldsymbol{\delta}} = (-\hat{\delta}_1, -\hat{\delta}_4 + \hat{\delta}_2, -\hat{\delta}_4, -\hat{\delta}_1 + \hat{\delta}_3)^T$ represents the excess noise of our C_Z gate. In the ideal case with $r \to \infty$, the noise term $\hat{\boldsymbol{\delta}}$ vanishes and a perfect C_Z operation is achieved. As the C_Z gate is an entangling gate, the presence of entanglement at the output for a product input state (in spite of the excess noise $\hat{\boldsymbol{\delta}}$) is crucial to prove the nonclassicality of our gate implementation. A sufficient condition for inseparability of a two-mode state is $\langle \Delta^2(g\hat{p}_\mu - \hat{x}_\nu)\rangle + \langle \Delta^2(g\hat{p}_\nu - \hat{x}_\mu)\rangle < g$ for some $g \in \mathbb{R}$ [22–24]. We show that this inequality is satisfied at the output for a two-mode vacuum input. In our case, $g = 3/4$ gives the minimal resource requirement, $e^{-2r} < 2/5$, corresponding to approximately -4.0 dB squeezing.

A schematic of our experimental setup is illustrated in Fig. 1(d). The light source is a continuous-wave Ti:sapphire laser with a wavelength of 860 nm and a power of 1.7 W. Four squeezed vacuum states are generated by four optical parametric oscillators (OPOs). We employ the experimental techniques described in Refs. [8,25] for the generation of the cluster state and the feedforward process, respectively. The resource squeezing is -5 dB on average and the detectors' quantum efficiencies are greater than 99%. The interference visibilities are 97% on average, while the propagation losses from the OPOs to the homodyne detectors are 3%–10%.

In the following, we show our experimental results. In Fig. 2, the input-output relation of our gate is investigated, using several coherent states for the input. In Fig. 3, the correlations at the output are determined, from which the presence of entanglement is verified. We use a spectrum analyzer to measure the power of the output quadratures. The measurement frequency is 1 MHz. The resolution and video bandwidths are 30 kHz and 300 Hz, respectively. All data in Fig. 2 are averaged 20 times, while those in Fig. 3 are averaged 40 times.

First, Fig. 2(a) shows the variances of the output quadratures when the two inputs are each in a vacuum state. In the case of the ideal C_Z gate, the variances of $\hat{x}_\mu$ and $\hat{x}_\nu$ remain unchanged and thus are equal to the shot noise level (SNL), while those of $\hat{p}_\mu$ and $\hat{p}_\nu$ are 3.0 dB above the SNL (2 times the SNL) as shown by the cyan lines. When the resource squeezing is finite, the output states are degraded by excess noise. We show as a reference the theoretical prediction for a vacuum resource [$r = 0$ in Eq. (3)] by green lines, where the variances of $\hat{x}_\mu$ and $\hat{x}_\nu$ are 4.8 dB above the SNL (3 times the SNL), while those of $\hat{p}_\mu$ and $\hat{p}_\nu$ 7.0 dB above the SNL (5 times the SNL). The experimental results of $\langle \Delta^2 \hat{x}_\mu\rangle$, $\langle \Delta^2 \hat{p}_\mu\rangle$, $\langle \Delta^2 \hat{x}_\nu\rangle$, and $\langle \Delta^2 \hat{p}_\nu\rangle$, shown by the red traces, are between cyan and green lines due to the finite resource squeezing. These correspond to 2.4, 4.6, 2.2, and 4.6 dB above the SNL, respectively. These results are consistent with the resource squeezing level of -5 dB, which leads to 2.1 dB for $\hat{x}_\mu, \hat{x}_\nu$ and 4.7 dB for $\hat{p}_\mu, \hat{p}_\nu$ above the SNL.

In order to verify the general input-output relations, we employ coherent input states [Figs. 2(b)–2(e)]. The powers of the amplitude quadratures are measured in advance, corresponding to 21.5 dB for mode α and 21.2 dB for mode β, respectively, compared to the SNL. Figure 2(b) shows the powers of the output quadratures as red traces when the input α is in a coherent state with a nonzero amplitude only in the $\hat{x}_\alpha$ quadrature; the input β is in a vacuum state. We observe an increase in powers of $\hat{x}_\mu$ and $\hat{p}_\nu$ caused by the nonzero coherent amplitude. On the other hand, $\hat{p}_\mu$ and $\hat{x}_\nu$ are not changed compared to the case of two vacuum inputs. In the same figure, the theoretical prediction is shown by blue lines. Clearly, the experimental results are in agreement with the theory. Similarly, Figs. 2(c)–2(e) show the results with a nonzero coherent amplitude in the $\hat{p}_\alpha$, $\hat{x}_\beta$, and $\hat{p}_\beta$ quadratures, respectively. We see the expected feature of the C_Z gate that the quadratures in modes α and β are transmitted to modes μ and ν with unity gain and $\hat{x}_\alpha$ and $\hat{x}_\beta$ are transferred to $\hat{p}_\nu$ and $\hat{p}_\mu$. We believe that the small discrepancies between our

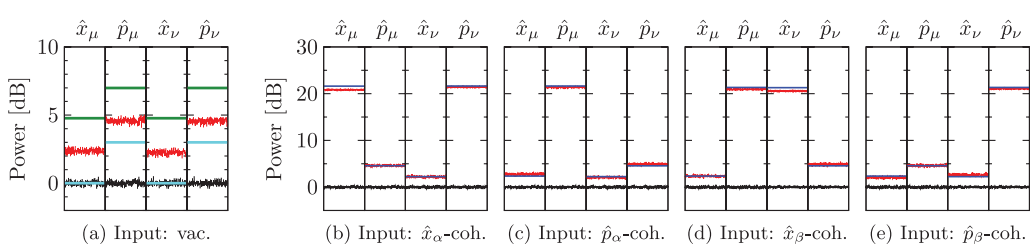

FIG. 2 (color). Powers at the outputs. (a) Variances of the output quadratures for vacuum inputs. The black and red traces correspond to the shot noise levels (SNLs) and output quadratures, respectively. The green lines show the theoretical prediction when no resource squeezing is available, while the cyan traces show the theoretical prediction for an ideal C_Z gate. (b)–(e) Powers of the output quadratures where $(\langle \hat{x}_\alpha\rangle, \langle \hat{p}_\alpha\rangle, \langle \hat{x}_\beta\rangle, \langle \hat{p}_\beta\rangle)$ are $(a, 0, 0, 0)$, $(0, a, 0, 0)$, $(0, 0, b, 0)$, and $(0, 0, 0, b)$, and where a and b correspond to 21.5 and 21.2 dB above the SNL, respectively. The blue lines show the theoretical prediction based on (a) and different input coherent amplitudes. vac., vacuum state; coh., coherent state.

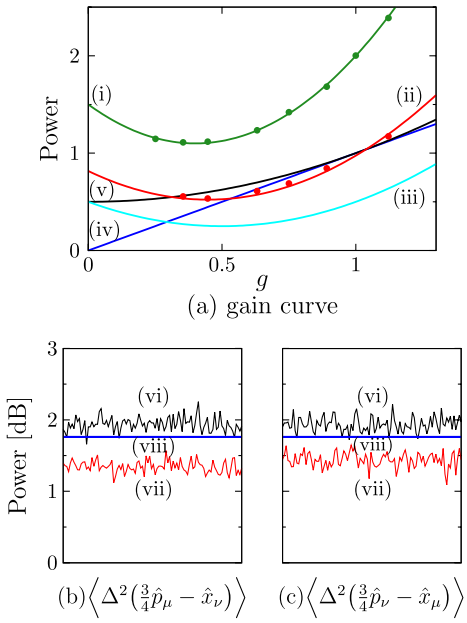

FIG. 3 (color online). Entanglement at the output. (a) Entanglement verification with several gains g. (i) Without resource squeezing, (ii) with -5 dB resource squeezing, (iii) with infinite resource squeezing (the ideal case), (iv) sufficient condition for entangling, and (v) the reference variance when two homodyne inputs are vacuum states. (b),(c) Variances of $\langle\Delta^2(g\hat{p}_\mu - \hat{x}_\nu)\rangle$ and $\langle\Delta^2(g\hat{p}_\nu - \hat{x}_\mu)\rangle$ at $g = 3/4$, respectively. 0 dB corresponds to the SNL. (vi) Reference where two homodyne inputs are vacuum states, (vii) the measurement results, and (viii) sufficient condition for entanglement.

experimental results and the theoretical predictions are caused by propagation losses and imperfect visibilities.

For assessing the entanglement at the output, we use two input states in the vacuum. The two homodyne signals are added electronically with a ratio of g^2:1 and 1:g^2 in power, by which $\langle\Delta^2(g\hat{p}_\mu - \hat{x}_\nu)\rangle$ and $\langle\Delta^2(g\hat{p}_\nu - \hat{x}_\mu)\rangle$ are measured.

Figure 3(a) shows the theoretical and experimental results for $\langle\Delta^2(g\hat{p}_\mu - \hat{x}_\nu)\rangle + \langle\Delta^2(g\hat{p}_\nu - \hat{x}_\mu)\rangle$ with several gains g. The sufficient condition for entanglement is that $\langle\Delta^2(g\hat{p}_\mu - \hat{x}_\nu)\rangle + \langle\Delta^2(g\hat{p}_\nu - \hat{x}_\mu)\rangle$ is less than g, shown by line (iv), for some $g \in \mathbb{R}$. When $g = 0.63$, 0.75, and 0.89, this criterion is satisfied in the experiment. The results without and with resource squeezing roughly coincide with the theoretical curves (i) and (ii), respectively. In particular, Figs. 3(b) and 3(c) show the results for the optimal gain $g = 3/4$. Traces (vi) show the reference for normalization when the two homodyne inputs are vacuum states. These levels correspond to $1 + g^2$ times the SNL. Traces (vii) show the measurement results for $\langle\Delta^2(g\hat{p}_\mu - \hat{x}_\nu)\rangle$ and $\langle\Delta^2(g\hat{p}_\nu - \hat{x}_\mu)\rangle$, which are -0.59 ± 0.02 dB and -0.50 ± 0.02 dB relative to traces (vi), respectively. Note that the error in determining the SNL is included in the above errors. Lines (viii) show the sufficient condition for entanglement, corresponding to the theoretical prediction with about -4.0 dB resource squeezing. The fact that traces (vii) are below lines (viii) proves that the output state is entangled. By normalizing the entanglement criterion, the obtained entanglement is quantified as follows:

$$\left\langle\Delta^2\left(\sqrt{g}\hat{p}_\mu - \frac{1}{\sqrt{g}}\hat{x}_\nu\right)\right\rangle + \left\langle\Delta^2\left(\sqrt{g}\hat{p}_\nu - \frac{1}{\sqrt{g}}\hat{x}_\mu\right)\right\rangle = 0.919 \pm 0.003 < 1, \quad \text{at } g = 3/4. \tag{4}$$

Note that traces (vi) and (vii) and line (viii) correspond to curves (v) and (ii) and line (iv) at $g = 3/4$, respectively.

In conclusion, we have experimentally demonstrated a fully cluster-based C_Z gate for continuous variables. In order to verify the essential property of the C_Z gate as an entangling gate, product two-mode input states were coupled with and processed through a four-mode cluster state, and entanglement at the output was clearly observed. In combination with our recent work on the experimental demonstration of single-mode Gaussian operations, all components for universal multimode Gaussian operations are now available in a one-way configuration. The quality of our C_Z gate is only limited by the squeezing level of the resource state, and the recently reported, higher levels of squeezing [26,27] would even allow us to realize multistep multimode one-way quantum computations. To achieve full universality when processing arbitrary multimode quantum optical states, the only missing ingredient is a single-mode non-Gaussian gate.

This work was partly supported by PDIS, GIA, G-COE, APSA, and FIRST commissioned by the MEXT of Japan, ASCR-JSPS, and SCOPE program of the MIC of Japan. R. U. acknowledges support from JSPS. P. v. L. acknowledges the Emmy Noether program of the DFG.

[1] R. Raussendorf and H. J. Briegel, Phys. Rev. Lett. **86**, 5188 (2001).
[2] J. Zhang and S. L. Braunstein, Phys. Rev. A **73**, 032318 (2006).
[3] N. C. Menicucci *et al.*, Phys. Rev. Lett. **97**, 110501 (2006).
[4] A. Furusawa and P. van Loock, *Quantum Teleportation and Entanglement* (Wiley-VCH, Berlin, 2011).
[5] S. Lloyd and S. L. Braunstein, Phys. Rev. Lett. **82**, 1784 (1999).
[6] P. van Loock, C. Weedbrook, and M. Gu, Phys. Rev. A **76**, 032321 (2007).
[7] X. Su *et al.*, Phys. Rev. Lett. **98**, 070502 (2007).
[8] M. Yukawa *et al.*, Phys. Rev. A **78**, 012301 (2008).
[9] P. van Loock, J. Opt. Soc. Am. B **24**, 340 (2007).
[10] R. Ukai *et al.*, Phys. Rev. A **81**, 032315 (2010).
[11] Y. Miwa *et al.*, Phys. Rev. A **80**, 050303(R) (2009).
[12] A. Furusawa *et al.*, Science **282**, 706 (1998).
[13] R. Ukai *et al.*, Phys. Rev. Lett. **106**, 240504 (2011).
[14] S. Sefi and P. van Loock, Phys. Rev. Lett. **107**, 170501 (2011).
[15] S. L. Braunstein, Phys. Rev. A **71**, 055801 (2005).

[16] M. Reck *et al.*, Phys. Rev. Lett. **73**, 58 (1994).
[17] Y. Wang *et al.*, Phys. Rev. A **81**, 022311 (2010).
[18] W. B. Gao *et al.*, Proc. Natl. Acad. Sci. U.S.A. **107**, 20 869 (2010).
[19] D. Gottesman and I. L. Chuang, Nature (London) **402**, 390 (1999).
[20] For deriving this fact, we must only consider the commutation relation between the C_Z interaction and the feed-forward displacements in the teleportations.
[21] Y. Miwa *et al.*, Phys. Rev. A **82**, 032305 (2010).
[22] L. M. Duan *et al.*, Phys. Rev. Lett. **84**, 2722 (2000).
[23] P. van Loock and A. Furusawa, Phys. Rev. A **67**, 052315 (2003).
[24] J. Yoshikawa *et al.*, Phys. Rev. Lett. **101**, 250501 (2008).
[25] M. Yukawa, H. Benichi, and A. Furusawa, Phys. Rev. A **77**, 022314 (2008).
[26] M. Mehmet *et al.*, Phys. Rev. A **81**, 013814 (2010).
[27] Y. Takeno *et al.*, Opt. Express **15**, 4321 (2007).